Light Scattering Measurements of the Repetitive Supersonic Implosion of a Sonoluminescing Bubble

Bradley P. Barber and Seth J. Putterman
Physics Department, University of California, Los Angeles, California 90024
(Received 14 September 1992)

Light scattering is used to measure the dynamics of the repetitive collapse of a sonoluminescing bubble of gas trapped in water. It is found that the surface of the bubble is collapsing with a supersonic velocity at about the time of light emission which in turn precedes the minimum bubble radius by about 0.03% of the period of the acoustic drive. These observations suggest that the shedding of an imploding shock mediates between the bubble collapse and light emission.

PACS numbers: 78.60.Mq, 43.25.+y, 42.65.Re, 47.40.−x

When a gas bubble is trapped in a fluid by a strong sound field it undergoes wildly nonlinear oscillations that can concentrate the average sound energy by over 12 orders of magnitude so as to create UV light [1] (sonoluminescence or SL). During the rarefaction part of the acoustic cycle the bubble absorbs energy from the sound field and its radius expands from an ambient value R_0 to a maximum value R_m. The subsequent compressional portion of the imposed sound field causes the bubble to collapse in a runaway fashion (first anticipated by Rayleigh [2]). The resulting excitation (heating) of the bubble contents (surface) leads to the emission of a pulse of light as the bubble approaches a minimum radius R_c. For various experimental parameters the pulse width is less than 50 ps and the peak powers are over 30 mW [1,3].

To date there is no explanation of how the flash width can be 6 orders of magnitude faster than the acoustic frequency, nor do we have an understanding of the parameters which determine the limits of the energy concentration that can be achieved. Toward this end we have set out to measure the detailed temporal evolution of the bubble radius [i.e., $R(t)$] and to compare it to the hydrodynamic theory of cavitation (the so-called Rayleigh-Plesset or RP equation [4]).

We find that (a) just before the minimum radius is reached the implosion velocity exceeds Mach-1 relative to the gas (for an acoustic period of 37.7 μs Mach-1 is reached about 10 ns before R_c); (b) the SL light is also emitted just prior to the minimum (about 5–10 ns prior to R_c); (c) R_m is about 40 μm and R_0 is about 4 μm which are much smaller than assumed or measured in previous works [5]; (d) hydrodynamics, in particular the RP equation, provides an excellent picture of the expansion phase of the bubble as well as the preliminary stages of the collapse; (e) at low sound fields the bubble can be trapped in a non-light-emitting state where its bounces are accurately described by fluid mechanics over the entire period of the motion.

The overall picture of bubble motion and SL emission is summarized by Fig. 1, which shows the intensity of light recorded by a single photomultiplier tube (PMT). The bubble is illuminated by a 1-mW HeNe laser and the tube records the sum of the SL and scattered light. The broad negative going peaks are due to the increase in scattered laser light as the bubble expands to R_m. The sharp spikes which follow the sudden drop in R are due to SL. Despite the catastrophic nature of the collapse, the SL emission can repeat with a jitter of less than 50 ps out of the sound field period which here is about 35 μs [3]. Use of faster detectors shows that the width of the SL spike is actually less than 50 ps [3].

Our goal now is to zoom in on the collapse and present measurements of bubble radius as a function of time. To go from voltage (or light intensity) to radius requires using the Mie theory of light scattering [6]. The dimensionless parameter which characterizes the light scattering is $\alpha = 2nR\pi/\lambda$, where n is the index of refraction (for water $n = 1.33$ and air is reckoned to unity) and λ is the

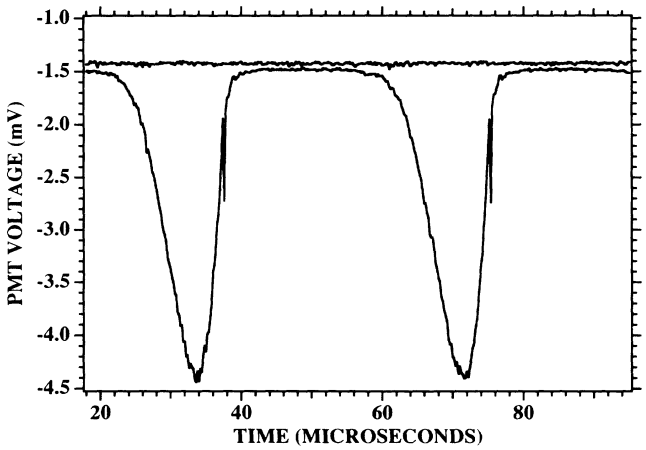

FIG. 1. Phase of emission of synchronous sonoluminescence: Intensity of light recorded on a photomultiplier tube as a function of time. The PMT records both the scattered laser light and the emitted SL from a single bubble trapped on a sound field. The broad negative peaks are due to the passage of the bubble through its maximum radius. The sharp peaks are due to SL, which is clearly emitted at or near the moment of bubble collapse. The horizontal line indicates the noise level in the absence of a bubble. The signal-to-noise ratio is not as good here as for Figs. 3 and 4 because the laser intensity and PMT have been chosen to make the SL apparent.

wavelength of imposed laser light (632.8 nm). In the WKB or ray optics limit [7] the intensity of light scattered by a spherical bubble of radius R is proportional to R^2 for all scattering angles. Application of the exact Mie scattering formulas indicates that the classical limit is approached rather slowly. In Fig. 2, $R=20$ μm (so α for water is 264), yet the exact Mie result exhibits many fringes when compared with the ray optics limit. As R varies, the exact formula for light scattered into a fixed angle goes roughly as the square of the radius but shows large variations due to the fringes moving through the angle.

In our experiments this problem is avoided by collecting light with a short focal length lens that spans 46°-94° from the forward direction. For this arrangement the fringes get averaged out and our calculation of the scattered intensity into this solid angle fits R^2 within 10% for radii $R>2$ μm and within 20% for $R>1$ μm. This angular region was chosen by a desire to stay away from (1) directly forward where the average is least effective and (2) backscatter where the intensity is orders of magnitude smaller. To reduce the detection of light scattered from impurities in the liquid an aperture is placed at the image of the bubble. A high gain PMT (Hamamatsu R2027) detects the light scattered out of a 10-mW laser. A second PMT captures the SL flash and triggers the detection. As we have mentioned, the tiny jitter in the time between SL flashes suggests that they be used to fix the zero of time. Appropriate filters are used to reduce the intensity of the laser relative to the SL for the trigger tube and vice versa for the signal tube.

The dynamic range of the PMT is not great enough to detect the bright and dim parts of the scatter in a single sweep. A pulse delay generator (SRS DG535) accepts the trigger and is used to trigger an acousto-optic (AO) modulator and a 250-MHz digital oscilloscope (HP 54510) operating in the repetitive mode. The AO modulator is used so that the laser can be interrupted during the bright expansion of the buble, allowing a high gain PMT to detect the dimmer parts of the oscillation without suffering damage during the expansions. The bubble is trapped at the center of a 100-ml quartz sphere filled with distilled, degassed water and driven by two piezoelectric transducers cemented to its outer wall.

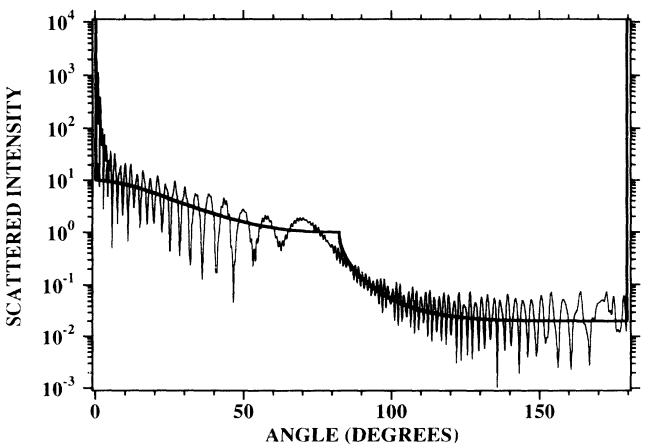

FIG. 2. Intensity of light as a function of angle of scattering: Compares the exact Mie theory (jagged curve) to the WKB or ray optics limit (smooth curve) for a 20-μm air bubble in water illuminated by a HeNe laser. The intensity is normalized such that geometric reflection from a mirrorlike sphere gives an intensity of 1.

The bubble radius is proportional to the square root of the PMT voltage $V(t)$ corrected for the background scatter $V(R=0)$ which is present when the laser and PMT are on but there is no bubble present (i.e., $R(t)\propto T(t)=[V(R=0)-V(t)]^{1/2}$). To find the constant of proportionality requires an absolute calibration for at least one point. This is achieved by matching a numerical calculation of the hydrodynamic theory of the bubble motion to that portion of the cycle where hydrodynamics must be valid. This ranges from the beginning of the growth of the bubble to the point where the collapse approaches, say, Mach-0.1. Two parameters, R_0 and the amplitude of the acoustic drive pressure P_a', determine the solution to the hydrodynamic theory of bubble motion [4]:

$$R\ddot{R}+\tfrac{3}{2}\dot{R}^2=[P_g(R)-P_a(t)-P_0]/\rho + (R/\rho c)d[P_g(R)-P_a(t)]/dt-4\nu\dot{R}/R\,, \tag{1}$$

where ν is the kinematic viscosity; ρ,c are the fluid density and sound velocity; P_0,P_g are the ambient and gas pressures; the acoustic field is given by $P_a=P_a'\sin\omega_a t$, where ω_a is the acoustic frequency; and we employ the van der Waals adiabatic equation of state:

$$P_g=P_0R_0^{3\gamma}/(R^3-a^3)^\gamma\,, \tag{2}$$

where γ is the ratio of specific heats and we see that $P_g=P_0$ when $R=R_0$. Equation (1) is the RP equation modified to include acoustic radiation damping and the van der Waals hard core a (for air $R_0/a\approx 8.5$) and surface tension has been neglected. The data $T(t)$ have a characteristic ratio of R_m to R_0. For a given ambient size bubble this ratio can be achieved by varying P_a' in the solution to Eq. (1) [8]. To find the correct ambient size the rate of expansion in $T(t)$ is matched. There is a unique R_0 and P_a' which will best match the data. Figure 3(a) shows that these matches are quite remarkable. The drive pressure of 1.3 atm is consistent with our measurements [3] and R_m is consistent with our upper bound estimates using a microscope. Once a match is found we have $R(t)=T(t)R_m/T_m$, where T_m is the value of T at R_m (this defines the heretofore undetermined proportionality constant between scattered intensity and R^2). When data were taken near the minimum of the first collapse we used the same experimental configuration but in-

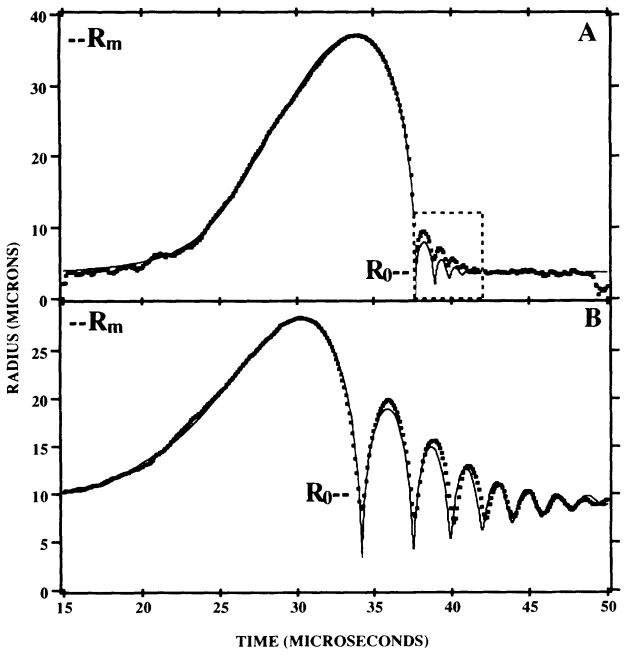

FIG. 3. Bubble radius as a function of time: in (a) the points are experimental data for a sonoluminescing bubble and the line is a simulation of Eqs. (1) and (2) for $R_0=4.5$ μm, $P_a'=1.325$ atm, $c=1481$ m/s, $\omega_a/2\pi=26.5$ kHz, and $\nu=0.07$ cm^2/s (relative to the noise floor the maximum radius corresponds to a signal of 4.1 mV); in (b) are shown data for a *non-light-emitting* bubble. The line here is a simulation using $R_0=10.5$ μm, $P_a'=1.075$ atm, and the same c, ω_a, and ν as used in (a).

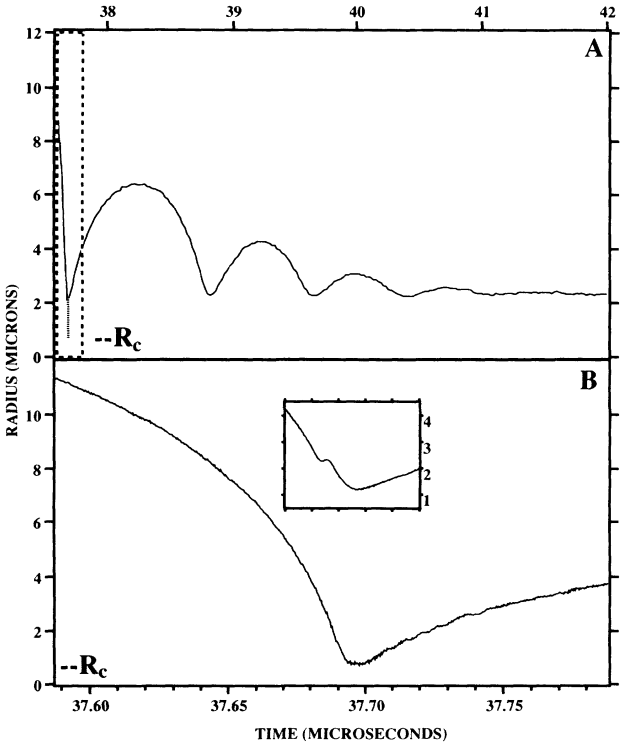

FIG. 4. Details of bubble radius vs time: (a) Blowup of the boxed region in 3(a) showing the breathing bounces of the bubble after the emission of SL. An extrapolation indicates the location of R_c as is resolved in (b) which shows the moment of collapse and is a blowup of the boxed region in (a). Inset: A different run where a laser line filter was not used; the bump prior to R_c is due to SL. The calibration for these figures is 60 μm/$\sqrt{\text{V}}$. (a),(b) A bubble with $R_0=3.25$ μm, $P_a'=1.375$ atm.

creased the gain G on the PMT as described above. The same constant of proportionality is used but an extra correction must be made for the gain of the PMT. In this case,

$$R(t)=T(t)[R_m/T_m]_s[G_s/G]^{1/2}, \tag{3}$$

where the subscript s denotes values calibrated via the computer simulation of the RP equation.

Figure 4(a) shows the breathing bounces made by the bubble after the light is emitted. This is a blowup of the region shown in Fig. 3(a). The period of these bounces is about 1 μs, which according to the equation for the frequency of breathing resonances [$\omega_0^2\approx 3(\rho_g/\rho)c_g^2/R_0^2$, where ρ_g,c_g are the density and speed of sound of the gas] implies an average radius of 3.5 μm, in good agreement with the calibration of the data via Eq. (1). The bounces as well as the ambient radii are far smaller than those reported previously [5]; we also find that the bubble radius is a constant for a sizable portion of the acoustic period that precedes its being recharged. Figure 4(b) shows the supersonic collapse of the trapped bubble. It is a blowup of the region shown in Fig. 4(a). As the bubble accelerates, its Mach number reaches unity about 10 ns before the minimum (note Mach-1 $=0.345$ μm/ns for $R\geq R_0$). The slow velocity of the wall of the bubble as R increases past R_c is due to the radiation of sound energy and the shedding of a shock that occurs just before R_c. The rise time of the R2027 PMT is 2.5 ns and the trigger jitter was measured to be less than 400 ps.

According to Eqs. (1) and (2) the bubble should collapse to about 0.5 μm. That this is not the case may be explained by the release of an imploding shock wave (not contained in the current hydrodynamic theories to cavitation, though it has been mentioned [9]). The reaction of the shock back onto the fluid-gas interface can cushion the collapse. Further evidence for the generation of an imploding shock is provided by the inset to Fig. 4(b). These data were obtained by removing the laser line pass filter used to acquire Fig. 4(b). In the inset the (ultraviolet) emission due to SL now appears as a bump on top of the (red) signal generated by the laser scatter. It appears that the SL is emitted about 5–10 ns prior to R_c. This effect can also be understood in terms of the release of an imploding shock which then generates the SL as well as slowing down the collapse of the bubble as described above. Finally, note that the weak 6-ns modulation of the bubble motion after R_c is reached. More detailed experiments should determine whether this is due to the rattling

of the shock inside the bubble.

Key to our plotting of the experimental data is the fact that the light is scattered by the bubble-liquid interface. In practice the imploding shock surface should also be a source of scattering. However, we expect this effect to be small because the area of the shock is small. Outgoing shocks in the liquid should be relatively weak (due to the higher sound velocity) so they also have a small scattering cross section. Key to our ability to resolve the light scattering from such a small object on such a rapid time scale is the existence of the stable, repetitive form of SL, the development of which is reported in Ref. [5] (see also [1,3]). Transient SL which occurs in uncontrolled distributions of cavitating bubbles is reviewed in Ref. [10].

Figure 3(b) shows the breathing motion of a bubble ($R_0 = 10.5$ μm) in a sound field whose amplitude is not large enough to generate SL ($P_a' = 1.075$ atm). The entire motion is well described by Eq. (1). The role of mass diffusion and P_a' in determining R_0 is discussed in Ref. [8]. Between the bouncing and SL regimes of Figs. 3(a) and 3(b), respectively, lies a region of "dancing instability" that has been ascribed to the parametric excitation of aspherical surface waves [5]. Throughout this paper we have assumed that the bubble motion is radial.

In conclusion, we have shown that light scattering measurements can resolve, on a nanosecond time scale, the supersonic motion of a bubble as its radius varies between 1 and 40 μm. These data indicate that SL is due to the excitation which accompanies a strong imploding shock wave that is shed by a gas-filled bubble as it collapses at a supersonic velocity. The recharging of the bubble as well as its approach to a sonic velocity is described well by Eqs. (1) and (2). Implicit in the equation of state [Eq. (2)] is the assumption that the gas pressure in the bubble is independent of position. This is true for $\dot{R}/c_g \ll 1$ [8]; but as $\dot{R}$ approaches c_g modulations and discontinuities can form. The unification of Eq. (1) to include the shedding of an imploding shock remains to be carried out. For an ideal shock the temperature at the origin of the bubble will go to infinity [11]. Thus mechanisms which damp the shock and lead to a finite thickness constitute an essential ingredient in determining the limits of energy concentration that can be achieved with SL [8].

This research is supported by the U.S. Department of Energy, Division of Advanced Energy Projects. We thank Hamamatsu for the gift of various photomultiplier tubes. We acknowledge valuable discussions with Tom Erber, B. I. Halperin, Ritva Löfstedt, Andrés Larraza, Arjun Yodh, and David Plant. We thank Robert Hiller for independently verifying key aspects of our experimental procedure.

[1] R. Hiller, S. J. Putterman, and B. P. Barber, Phys. Rev. Lett. **69**, 1182 (1992).

[2] Rayleigh, Philos. Mag. **34**, 94 (1917).

[3] B. Barber and S. Putterman, Nature (London) **352**, 318 (1991); B. P. Barber, R. Hiller, K. Arisaka, H. Fetterman, and S. J. Putterman, J. Acoust. Soc. Am. **91**, 3061 (1992).

[4] A. Prosperetti, Rend. S.I.F. **93**, 145 (1984); B. Noltingk and E. Neppiras, Proc. Phys. Soc. London B **63**, 674 (1950).

[5] D. F. Gaitan, L. A. Crum, C. C. Church, and R. A. Roy, J. Acoust. Soc. Am. **91**, 3166 (1992); D. F. Gaitan and L. A. Crum, J. Acoust. Soc. Am., Suppl. 1, **87**, S141 (1990).

[6] H. C. Van de Hulst, *Light Scattering by Small Particles* (Wiley, New York, 1957); M. Kerker, *The Scattering of Light and other Electromagnetic Radiation* (Academic, New York, 1969); W. J. Wiscombe, Appl. Opt. **19**, 1505 (1980); P. Marston, Appl. Opt. **30**, 3479 (1991); J. V. Dave, IBM J. Res. Dev. **13**, 302 (1969).

[7] G. E. Davis, J. Opt. Soc. Am. **45**, 572 (1955).

[8] R. Löfstedt, B. P. Barber, and S. J. Putterman (to be published).

[9] P. Jarman, J. Acoust. Soc. Am. **32**, 1459 (1960); L. J. Trilling, J. Appl. Phys. **23**, 14 (1952); F. I. Bykovtsev and G. S. Rozarenov, Fluid Dyn. Sov. Res. **10**, 322 (1975); R. Löfstedt, B. P. Barber, R. Hiller, and S. J. Putterman, J. Acoust. Soc. Am. **91**, S2331 (1992); W. C. Moss, D. B. Clarke, R. A. Day, and J. W. White (to be published).

[10] A. J. Walton and G. T. Reynolds, Adv. Phys. **33**, 595 (1984).

[11] L. D. Landau and E. M. Lifshitz, *Fluid Mechanics* (Pergamon, New York, 1987), 2nd ed.